

Application of a Monte Carlo integration method to collision and coagulation growth processes of hydrometeors in a bin-type model

Yousuke Sato,¹ Teruyuki Nakajima,¹ Kentaroh Suzuki,² and Takamichi Iguchi¹

Received 5 October 2008; revised 27 February 2009; accepted 11 March 2009; published 13 May 2009.

[1] New algorithms for calculating the collision-coagulation growth process of hydrometeors were developed and implemented into a bin cloud microphysics model in order to improve its computational efficiency. Computation of collision-coagulation growth is a bottleneck in the bin-type cloud microphysics calculation that takes a large amount of computing time. Improvement in the efficiency of the process can significantly reduce computing time. In this study, a new stochastic algorithm was developed and implemented into the collision-coagulation growth process of a nonhydrostatic cloud model. Simulations showed that the computing time was reduced by about 90%. We verified that the error range of the simulation results from the new scheme is much smaller than the internal variability involved in the traditional bin-type model and also in the real atmosphere. The newly developed scheme was implemented into the mesoscale operational model of the Japan Meteorological Agency. The precipitation field was accurately simulated in a numerical weather prediction simulation.

Citation: Sato, Y., T. Nakajima, K. Suzuki, and T. Iguchi (2009), Application of a Monte Carlo integration method to collision and coagulation growth processes of hydrometeors in a bin-type model, *J. Geophys. Res.*, 114, D09215, doi:10.1029/2008JD011247.

1. Introduction

[2] Clouds, which cover about 70% of the Earth's surface [Rossow and Schiffer, 1999], play a critical role in the atmosphere through various interaction processes such as latent heat release, radiation and water circulation. In particular, the recent attention of the climate research community to cloud perturbation by anthropogenic aerosols demands extensive simulations of detailed cloud microphysics. In such simulations, bin-type cloud models have been used to study the detailed modification of the size distribution of cloud droplets and aerosol particles [e.g., Khain *et al.*, 2005; Lynn *et al.*, 2005]. The satellite-derived signature of aerosol-cloud interaction with a significant reduction of the effective droplet radius has also been successfully simulated by these bin-type models [Suzuki *et al.*, 2006; Iguchi *et al.*, 2008].

[3] The bin-type model, however, takes a large amount of computing time and is difficult to be used for simulation of large-scale areas and/or for many runs in sensitivity studies. So far the model has therefore been used only for idealized and mesoscale regional case studies [e.g., Khain and Sednev, 1996; Takahashi and Kawano, 1998; Lynn *et al.*, 2005; Iguchi *et al.*, 2008]. On the other hand, Shima *et al.* [2009] developed the super-droplet method, which can treat

detailed cloud microphysics and have potential to reduce computational cost of cloud physics.

[4] Table 1 shows an example of CPU time taken by microphysical processes in the bin model of Suzuki *et al.* [2006]. The table indicates that more than 98% of the total CPU time is used by the condensation and the collision-coagulation processes, although different cases depend on the algorithms adopted by each bin-type model. In order to increase the computational efficiency, Bott [1998, 2000] proposed a flux method to reduce the numerical diffusion in the collision-coagulation processes by using a mass density distribution function, instead of the number density distribution function and using an accurate interpolation to solve the stochastic collision equation. Suzuki [2004] proposed a base function method to reduce the numerical diffusion by expanding the size distribution by a series of orthogonal functions. In spite of these improvements, the computational cost of bin-type models is still high.

[5] In this article, we propose a stochastic size integration method for the collision-coagulation process of a bin type cloud model. And the purpose of this article is to develop a numerically efficient method to approximate the traditional bin method which is widely used by many researchers, in order to reduce the computation cost. We present the model description in section 2, calculation results in sections 3, 4, and 5 and the discussion in section 6.

2. Model Description

[6] The collision-coagulation growth of hydrometeors in cloud is calculated by solving the stochastic collection

¹Center for Climate System Research, University of Tokyo, Kashiwa, Japan.

²Department of Atmospheric Science, Colorado State University, Fort Collins, Colorado, USA.

Table 1. Example of the CPU Times and Contributions to the Total Time for Calculation of Cloud Microphysics Processes by a Bin-Type Model

Process	CPU Time (s)	Contribution to Total Time (%)
Nucleation	2.98	0.3
Freezing, melting	3.45	0.3
Condensation	808.39	70.9
Collision and coagulation	325.13	28.5
All	1139.95	100

equation (SCE) [e.g., Pruppacher and Klett, 1997; Khain et al., 2000]:

$$\frac{\partial f(m)}{\partial t} = 2 \int_0^{m/2} f(m')f(m-m')K(m', m-m')dm' - f(m) \int_0^{\infty} f(m'')K(m, m'')dm'', \quad (1)$$

where m is the mass of a hydrometeor particle, $f(m)$ is the number size distribution function (SDF) (number size concentration) and $K(m', m)$ is the collection kernel function determining the rate at which a particle of mass m' is collected by a particle of mass m . In order to solve (1), we adopt a logarithmically equidistant mass grid system following Bott [1998]. Following Berry [1967], a mass density function, $g(\eta)$, is introduced by

$$g(\eta) = m^2 f(m) \quad (\eta = \ln m). \quad (2)$$

Substituting $g(\eta)$ into (1), the SCE of the mass density function is written as

$$\frac{\partial g(\eta)}{\partial t} = 2 \int_0^{\eta_1} \frac{m^2}{m_c^2 m'} g(\eta') g(\eta_c) K(\eta', \eta_c) d\eta' - \int_0^{\infty} g(\eta) \frac{K(\eta, \eta'')}{m''} g(\eta'') d\eta'', \quad (3)$$

where $\eta_c = \ln(m_c)$; $m_c = m - m'$; $\eta_1 = \exp(\eta)/2$.

[7] Collision of a particle at a grid point i (i th bin), whose mass is m_i , with a particle at a grid point j (j th bin), whose mass is m_j , yields a change in the mass density functions at the i th and j th bins, g_i and g_j . It also produces a new particle with mass $m' = m_i + m_j$. This process is calculated as follows:

$$g_i(i, j) = g_i - g_i \frac{K(i, j)}{m_j} g_j \Delta\eta \Delta t = g_i - \Delta g_i, \quad (4a)$$

$$g_j(j, i) = g_j - g_j \frac{K(i, j)}{m_i} g_i \Delta\eta \Delta t = g_j - \Delta g_j, \quad (4b)$$

$$g'(i, j) = \Delta g_i + \Delta g_j,$$

$$(i, j = 1, 2, \dots, N_{\text{bin}}), \quad (4c)$$

where Δg_i and Δg_j are the masses lost from i th and j th bins by collision, respectively, and $g'_i(i, j)$ and $g'_j(i, j)$ are values of the mass density function after the collision at the i th and j th bin, respectively. $g'(i, j)$ represents the total mass increase of the particle system identified as the new particle m' after the collision. $\Delta\eta$ is the grid spacing of the logarithmically equidistant mass grid system, Δt is the time interval for numerical integration and N_{bin} is the number of bins. Supposing that the new particle mass is in a k th bin, i.e., $m_k < m' < m_{k+1}$, $g'(i, j)$ is decomposed into two contributions for k th and $k + 1$ st bins as in the scheme proposed by Bott [2000].

[8] The traditional bin method evaluates all the collision combinations, $N_{\text{bin}}C_2$, to solve (3) as follows:

$$\{g_l\}_{l=1,2,\dots,N_{\text{bin}}} = \sum_i^{N_{\text{bin}}-1} \sum_j^{N_{\text{bin}}} (\Delta g_i + \Delta g_j). \quad (5)$$

[9] On the other hand, in this study, we approximate (5) using a Monte Carlo integration (MCI) algorithm. This method does not calculate all combinations of bins, instead only some combinations are selected by uniform random numbers:

$$\{g_l\}_{l=1,2,\dots,N_{\text{bin}}} = \sum_{k_1=1, k_2=1}^M (\Delta g_{k_1} + \Delta g_{k_2}) \times w \quad w = \frac{N_{\text{bin}}C_2}{M}, \quad (6)$$

where M is the number of selected bin combinations and w is a weighting factor to compensate for the lack of mass change caused by the reduced number of combinations. Computational efficiency is improved by introducing the factor w compared to the traditional bin method.

[10] Equations (1), (5), and (6) assume collision and coagulation among particles of the same type of hydrometeor. We can extend these expressions to those for poly dispersions for different types of hydrometeors, such as the seven hydrometeor types identified in the Hebrew University Cloud Model [Khain and Sednev, 1996] as follows:

$$\frac{\partial f^{(\lambda)}(m)}{\partial t} = \sum_{\nu} \sum_{\mu} 2 \int_0^{m/2} f^{(\nu)}(m') f^{(\mu)}(m-m') \cdot K(m', m-m') dm' - f^{(\lambda)}(m) \sum_{\sigma} \int_0^{\infty} f^{(\sigma)}(m'') K(m, m'') dm'' \quad (7)$$

$$\begin{aligned} \{g_l^{(\lambda)}\}_{l=1,2,\dots,N_{\text{bin}}}^{\lambda=1,2,\dots,N_{\text{spc}}} &= \sum_{\mu} \sum_{\nu} \left[\sum_i \sum_j (\Delta g_i^{(\mu)} + \Delta g_j^{(\nu)}) \right] \\ &\approx \sum_{\lambda_1=1, \lambda_2=1}^L \sum_{k_1=1, k_2=1}^M \left[(\Delta g_{k_1}^{\lambda_1} + \Delta g_{k_2}^{\lambda_2}) \right] \times w, \quad (8) \\ &\left[w = \left(\frac{N_{\text{bin}}C_2}{M} \frac{N_{\text{spc}}^2}{L} \right) \right], \end{aligned}$$

where μ , ν , σ , and λ represent the type of hydrometeor, N_{spc} is the number of hydrometeor types and L is the number of hydrometeor types selected in the MCI. The quadruplex integration in (7) is reduced to a double summation in (8), so that the MCI introduces a significant benefit in the calculation time for the collision-coagulation process for poly dispersions including different types of hydrometeors. In summary, the computational efficiency is improved by random bin selection with ratio of $w_1 (= N_{\text{bin}} C_2 / M)$ and also by hydrometeor type selection with ratio of $w_2 (= N_{\text{spc}}^2 / L)$. The total computation time is therefore reduced by the factor $R_{\text{comp}} = 1/w_1 w_2$.

[11] In case of large w , the size distribution in the next time step can become negative when $g_i < \Delta g_i$ or $g_j < \Delta g_j$. In this case, we assure positive definiteness by the following procedure as proposed by *Bott* [1998]:

$$\begin{aligned} g_i(i, j) &= \max(g_i - \Delta g_i, 0) \\ g_j(j, i) &= \begin{cases} \max(g_j - \Delta g_j, 0) & (i \neq j) \\ g_j - \Delta g_j & (i = j) \end{cases} \end{aligned} \quad (9)$$

Our method is also different from traditional bin method in terms of calculation order regarding hydrometeor types and sizes of hydrometeor. Traditional bin methods calculate interaction of different hydrometeor types and different sizes by collision with specific order (e.g., first, collision of liquid drop and ice particle, second liquid drop and snow particle, next, liquid drop and graupel etc.). This can be invalid for collision process in nature if the natural collision process occurs randomly in terms of pairing of colliding particles and types. In our MCI, however, collision process is calculated by random order about hydrometeor type and size of hydrometeor because the order is selected by uniform random number. This may be more suitable to represent the stochastic nature of collision process in real clouds.

3. Results of Numerical Experiments With a Box Model

[12] In this section, we show the results of numerical simulations with the present MCI applied to a zero-dimensional box model, which calculates the development of SDF by only the collision-coagulation process. Simulated results are compared with the analytic solution of SCE [*Golovin*, 1963] and the results with Exponential Flux Method (EFM) [*Bott*, 2000]. We also evaluate the computational cost and error of the MCI.

[13] For the test simulation, we integrate the SCE over the total time of 7200 s with a time interval of $\Delta t = 1$ s. The SDF is discretized by $N_{\text{bin}} = 300$ size bins through uniformly dividing the logarithm of the hydrometeor's mass. Only one type of hydrometeor (water droplet) is considered. The initial size distribution is assumed to be the form of a gamma function:

$$f(m, t = 0) = \frac{L'}{\bar{m}} \exp\left(-\frac{m}{\bar{m}}\right), \quad (10)$$

where L' is the total cloud water content and \bar{m} is the mean droplet mass. The mean radius of hydrometeor \bar{r} can be

defined as $\bar{m} = (4/3) \pi \rho \bar{r}^3$ where ρ is the density of water. We assume $L' = 1 \text{ g m}^{-3}$ and $\bar{r} = 10 \text{ }\mu\text{m}$ in our simulation.

[14] Figure 1a compares the MCI result with the analytic solution for the Golovin kernel function $K(m', m) = (1.5 \times 10^{-3}) \times (m + m')$ [*Berry*, 1967]. It shows that the SDF obtained by the MCI are not smooth functions of mass of hydrometeor but this nonsmooth nature does not develop with time. The peak mode radii are same as those of analytic solution. And the maximum deviation from the analytic SDF at each time step remains similar to that of traditional method (not shown). The root mean square error in the SDF over the total time becomes less than that of the traditional bin method when $R (= 1/w_1)$ is larger than 0.031.

[15] Figures 1b and 1c compare the results of the MCI with the EFM using a realistic kernel called the hydrodynamic kernel:

$$\begin{aligned} K(m', m) &= \pi \{r(m) + r(m')\}^2 |V(m) - V(m')| \\ &\cdot E_{\text{col}}(m, m') E_{\text{coal}}(m, m'), \end{aligned}$$

where $V(m)$ and $r(m)$ are the terminal velocity and radius of a hydrometeor whose mass is m , respectively, and E_{col} and E_{coal} represent the collection and coalescence efficiencies, respectively. In this case, the MCI gives an appropriate SDF when $R (= 1/w_1 = M/N_{\text{bin}} C_2)$ is in the range from 0.056 to 1 as shown in Figures 1b and 1c. However, growth of hydrometeor becomes delayed (see Figure 1c) when R becomes as small as 0.031. A detailed study of the simulation results suggests that this delay begins when the compensation factor w in (6) becomes inadequately large, producing a significantly large value of Δg_{ij} which cannot be adequately corrected by (9). Therefore, R should be set as larger than 0.056 in the present MCI.

[16] Figures 2a and 2b show CPU time taken by the MCI as a function of R and $R_{\text{spc}} (= 1/w_2 = L/N_{\text{spc}}^2)$. The figure shows that the CPU time changes in proportion to R and R_{spc} . When R is one, the CPU time of the present method is larger than that of the traditional bin method due to the cost of generating random numbers. When R is 0.056, which is the minimum value of R required for appropriate results, the CPU time is about 10% of traditional bin method.

4. Comparison With the Traditional Bin Method Using a Two-Dimensional Model

[17] We also performed two-dimensional simulations in order to compare the results from the MCI and the traditional bin method. We selected two cases for simulation: a convective cloud case and a shallow stratus case generated by a warm bubble. We use a bin model developed by *Suzuki et al.* [2006]. The simulation domain is a two-dimensional area ($x - z$) of 30 km ($dx = 0.5$ km) in the horizontal direction and 15 km ($dz = 0.2$ km) in vertical direction for the convective cloud case, and 30 km ($dx = 0.5$ km) in horizontal and 5 km ($dz = 0.05$ km) in vertical direction for the stratus case. Initial conditions of wind shear, relative humidity and temperature as shown in Figure 3 are based on *Suzuki* [2004] for convective cloud and *Suzuki et al.* [2006] for stratus cloud, respectively. To trigger convection and cloud formation, a warm bubble is initially located as a

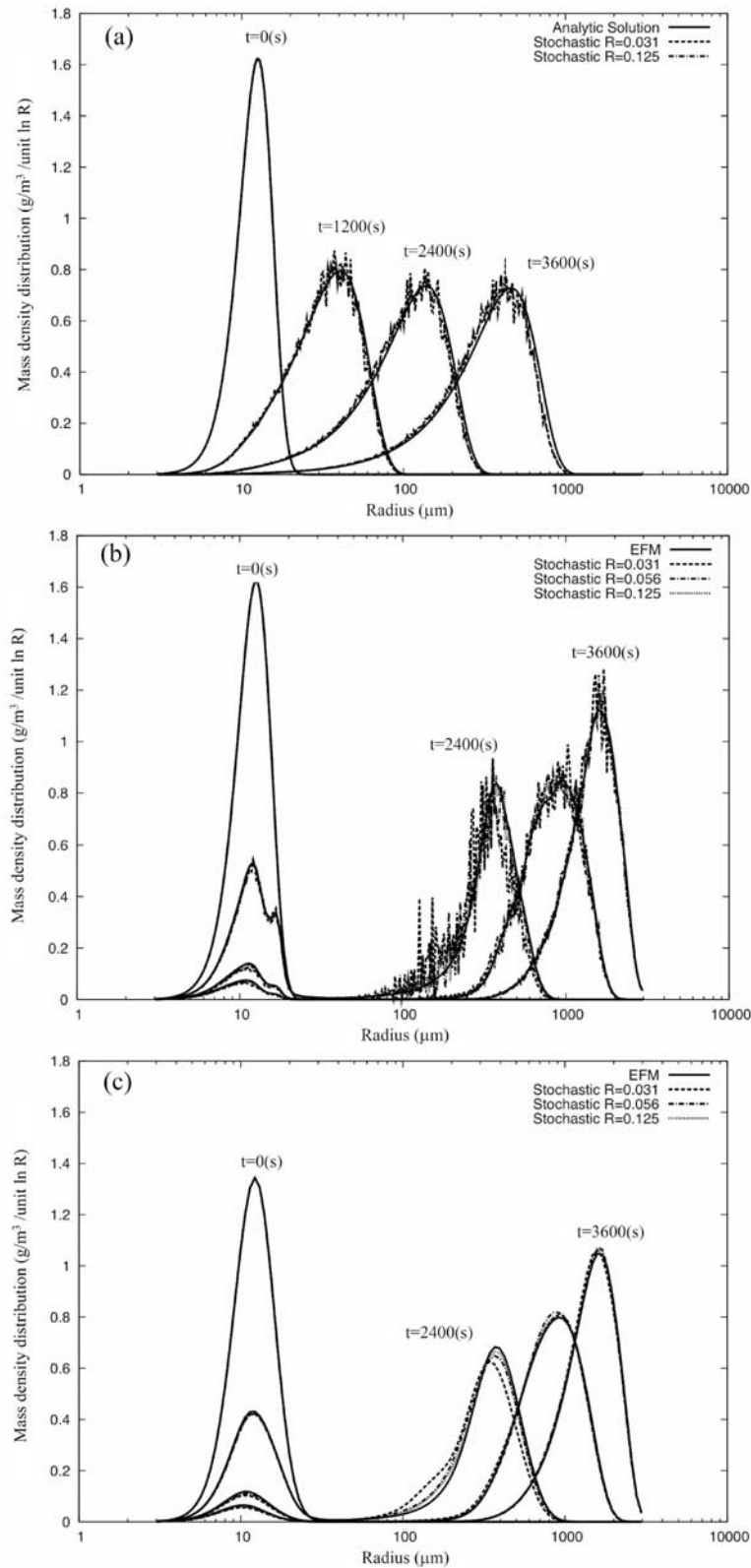


Figure 1. (a, b) Time evolution of the mass density size distribution (SDF) and (c) the smoothed result of Figure 1b. In Figure 1a, the solid line represents the analytic solution of the stochastic collection equation (SCE) [Golovin, 1963] and dashed lines and dash-dotted lines represent the numerical results obtained by the Monte Carlo integration (MCI) with $R = 0.031$ and 0.125 , respectively. In Figures 1b and 1c, solid lines represent the numerical results obtained by the traditional bin method, and dashed lines, dash-dotted lines, and dotted lines represent those obtained by the MCI with $R = 0.031$, 0.056 , and 0.125 , respectively.

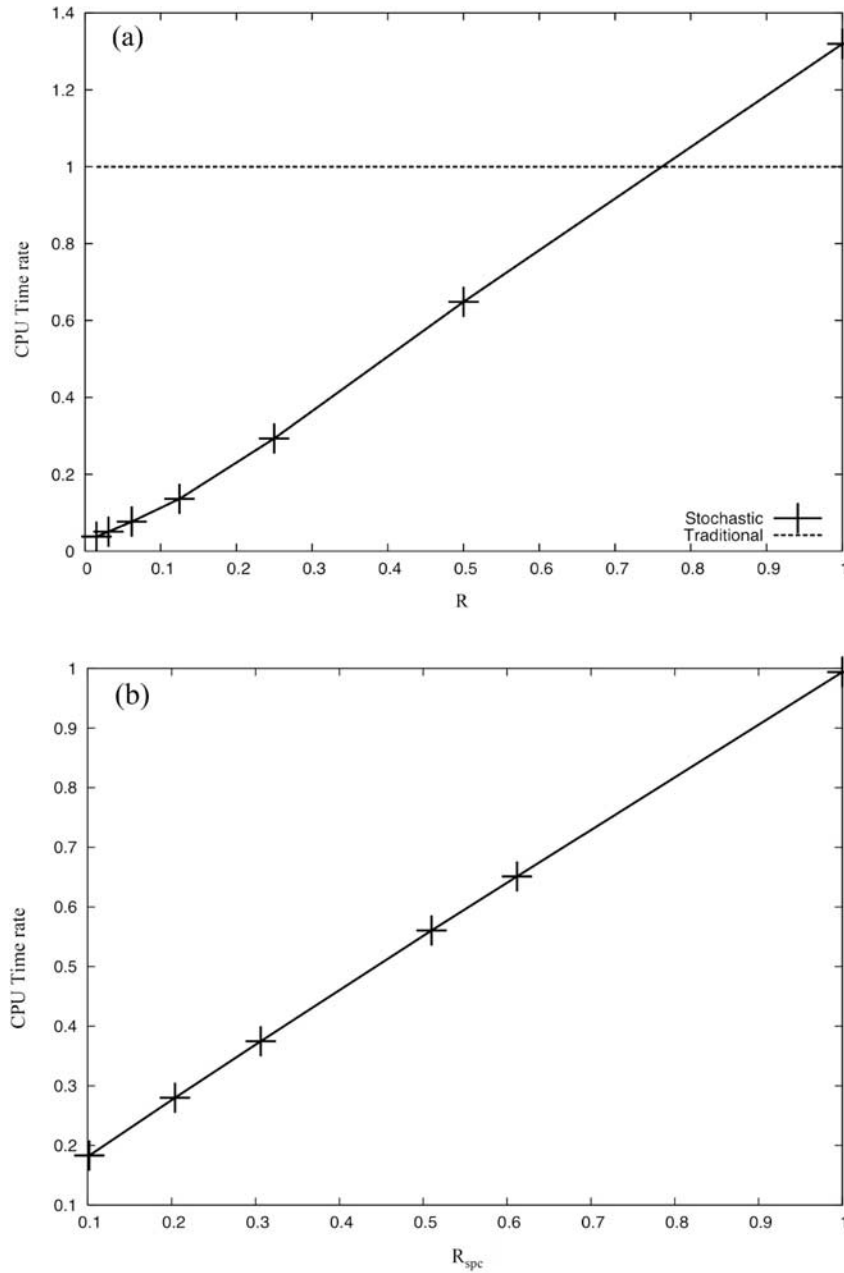


Figure 2. CPU times for the collision-coagulation processes, normalized by the CPU time for the traditional bin method, as functions of (a) R and (b) R_{spc} . Solid lines and dots are CPU times taken by the MCI, and dotted lines are those for the traditional bin method.

potential temperature perturbation $\Delta\theta$ following *Gallus and Rancic* [1996]:

$$\Delta\theta = \Delta\theta_0 \left(\frac{\pi}{2} \sqrt{\left(\frac{x - x_0}{x_r} \right)^2 + \left(\frac{z - z_0}{z_r} \right)^2} \right),$$

where $x_0 = 9$ km, $z_0 = 1$ km, $x_r = 5$ km, $z_r = 1$ km and $\Delta\theta = 1$ K for the convective cloud case, and $x_0 = 9$ km, $z_0 = 0.5$ km, $x_r = 5$ km, $z_r = 0.5$ km and $\Delta\theta = 1$ K for the stratus case. In the stratus simulation, we consider only warm processes because the cloud top temperature is always above 273 K. On the other hand, the convective cloud

simulation is performed including the ice phase process with the seven types of hydrometeors, i.e., cloud droplet, ice crystals (plate, column, dendrite), snow, hail and graupel. First, we set $R_{\text{spc}} = 1$ and various R values from 1 to 0.056, and we take an ensemble average of five experimental results where R are same but the seeded random numbers are different. We integrate for 7200 s (2 h) with a time step of $\Delta t = 1$ s. SDFs of hydrometeors are discretized into 60 size bins (i.e., $N_{\text{bin}} = 60$) by uniformly dividing the logarithm of the mass of hydrometeor. The range of hydrometeor size is defined as 3–3000 μm . We call 3–30 μm , 30–300 μm , and 300–3000 μm cloud, drizzle and rainwater, respectively.

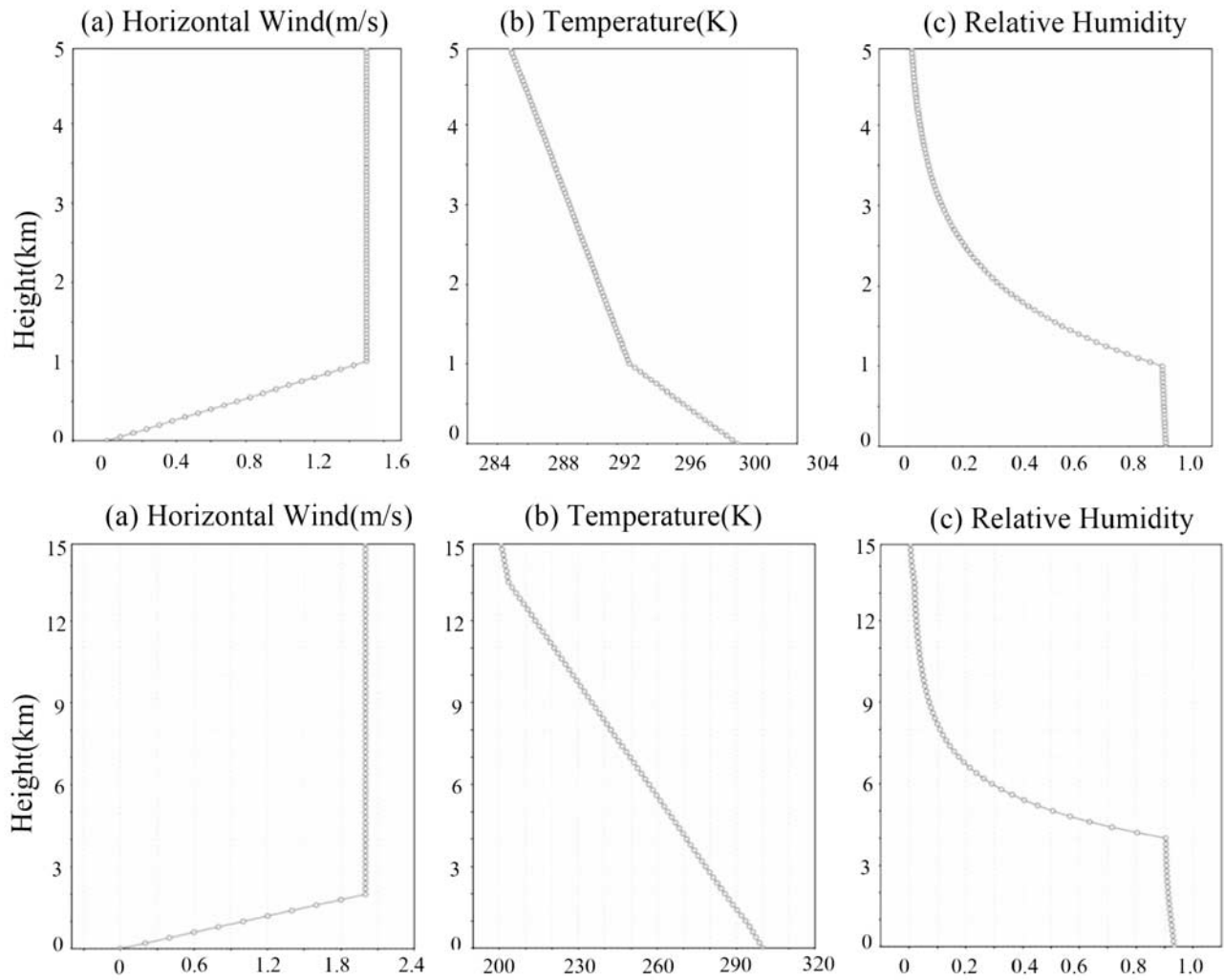


Figure 3. Initial conditions for atmospheric dynamics assumed for the two-dimensional numerical experiments: (a) horizontal wind, (b) temperature, and (c) relative humidity. (top) Stratus case; (bottom) convective cloud case.

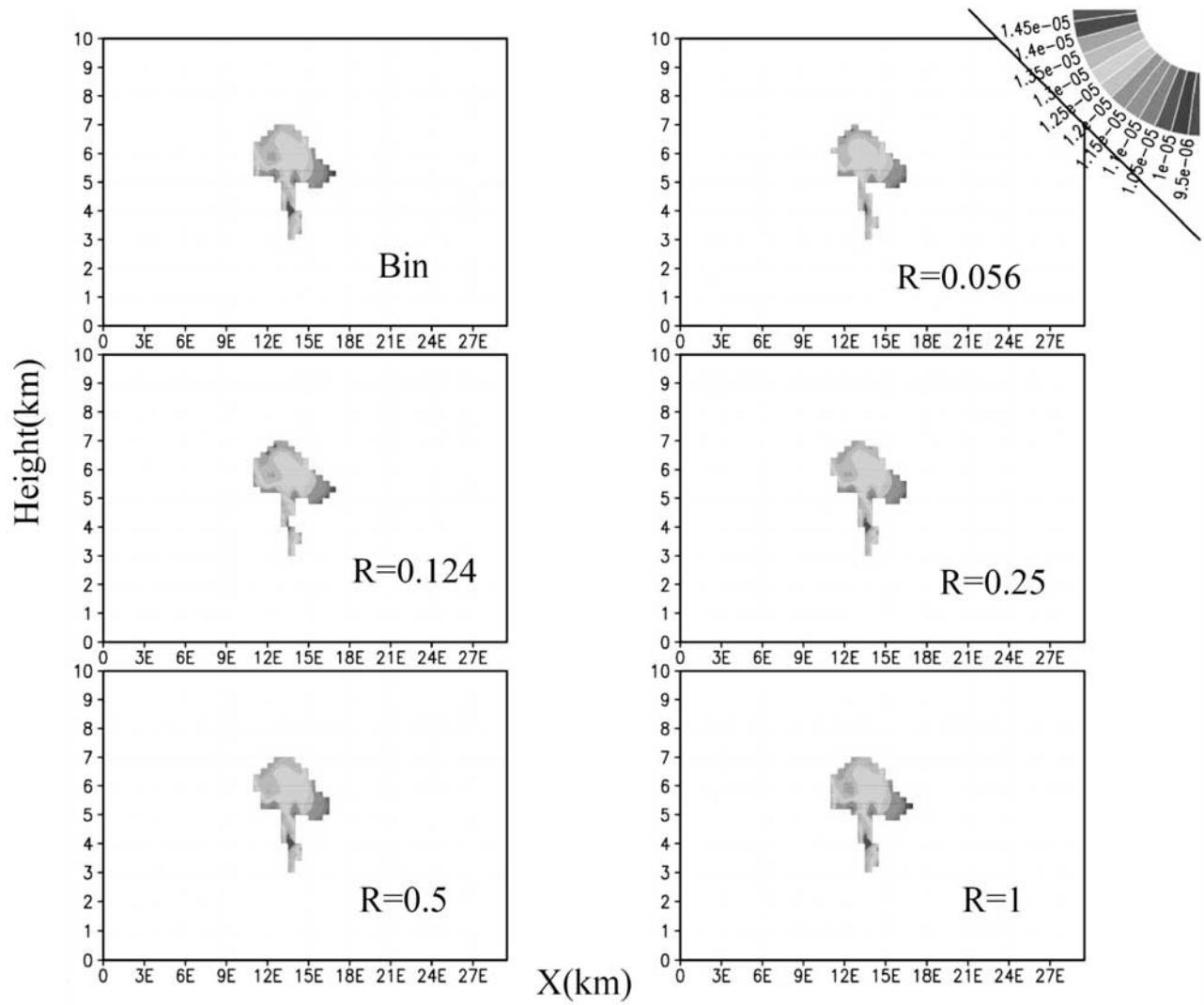


Figure 4. Horizontal distance-height sections of the cloud effective radius distribution formed by a warm bubble at $t = 60$ min in the convective cloud case for $R_{\text{spc}} = 1$ and various values of R . The panel labeled with “bin” represents the result of the traditional bin model.

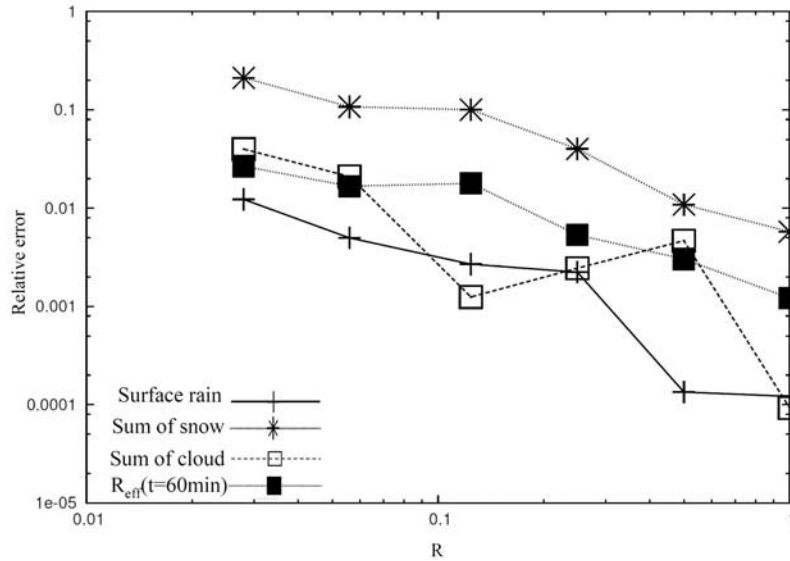


Figure 5. Relative errors of the MCI averaged over the whole simulation domain for time-integrated amounts of surface rain (crosses), cloud water content (open squares), snow water content (asterisks), and effective radius (solid squares) at $t = 60$ min.

[18] Figure 4 shows a snapshot of the cloud effective radius distribution for the convective cloud case 60 min after the start of the calculation. As expected from the previous tests, the present method gives results similar to the traditional bin method even if R is as small as 0.056. Figure 5 shows the relative error of the MCI from the result of the traditional bin method. The mean error of each set of simulations changes exponentially with R . Relative errors of the effective radius of cloud,

$$r_e = \frac{\int_{r=3\mu\text{m}}^{r=30\mu\text{m}} r^3 f(r) dr}{\int_{r=3\mu\text{m}}^{r=30\text{mm}} r^2 f(r) dr},$$

and the accumulated amount of cloud water content, integrated from the initial time to the end of simulation, are about 3% and that of surface rainfall is less than 1% when R is 0.056.

[19] Next, we change R_{spc} for a fixed R at 0.124. Figure 6 shows the accumulated amount of snow water content. When R_{spc} is less than one, the snow amount is either over- or underestimated, though it seems that there is no specific preference of R_{spc} values to cause either. The present method over/underestimates all ice phase hydrometeors, including ice, graupel and hail amounts, though not shown. Such over/underestimation is caused by a lack of mass transfer among some hydrometeor types in the MCI. If R_{spc} is smaller than one, there are some types of hydrometeors for which collision and coagulation processes are not calculated. As a result, some types of hydrometeors grow more than by the traditional method, while another type

does not grow fast enough. There are no preferred types and values of R_{spc} for over/underestimation as shown in Figure 6 because hydrometeors for calculation are randomly selected. Figure 7 shows relative errors of the MCI for various values of R_{spc} . The relative errors for all the hydrometeor types change exponentially with R_{spc} , as in the case of variable R .

[20] Figures 8 and 9 show a snapshot of the effective radius distribution and the relative error as a function of R , respectively, in the stratus case at $t = 60$ min. As in the simulation of the convective cloud case, the present method obtains results similar to the traditional bin method even if R is 0.056 (Figure 8) and the relative error changes exponentially with R (Figure 9). Figure 10 shows the spatially averaged SDF (Mass density distribution) at 60 min after the start of simulation calculated by traditional bin and MCI. These SDFs have complex forms with bimodal feature. It is shown that the SDFs with $R = 0.056$ and 0.124 have unsmoothed forms in second mode whereas the peak radii are same as the others, similar to the results with box model in section 3. This illustrates that the MCI can also reproduce complex forms of SDF (e.g., bimodal or trimodal SDF) similar to traditional bin methods even for two dimensional cases.

[21] Figure 11 shows the CPU time of the collision-coagulation process for the two-dimensional simulations. The slope of the fitted line for the stratus case (Figure 11b), 118 s, is smaller than 2291 s for the convective case (Figure 11a). This is because the collision and coagulation module is called more frequently in the convective case than in the stratus case, and also because, in convective cloud case, collisions between liquid particles and ice particles (e.g., ice crystals, snow, graupel and hail particles) are calculated since cloud top temperature of convective cloud is lower than 273 K. These results suggest that the more frequently the collision module is called, the stronger the

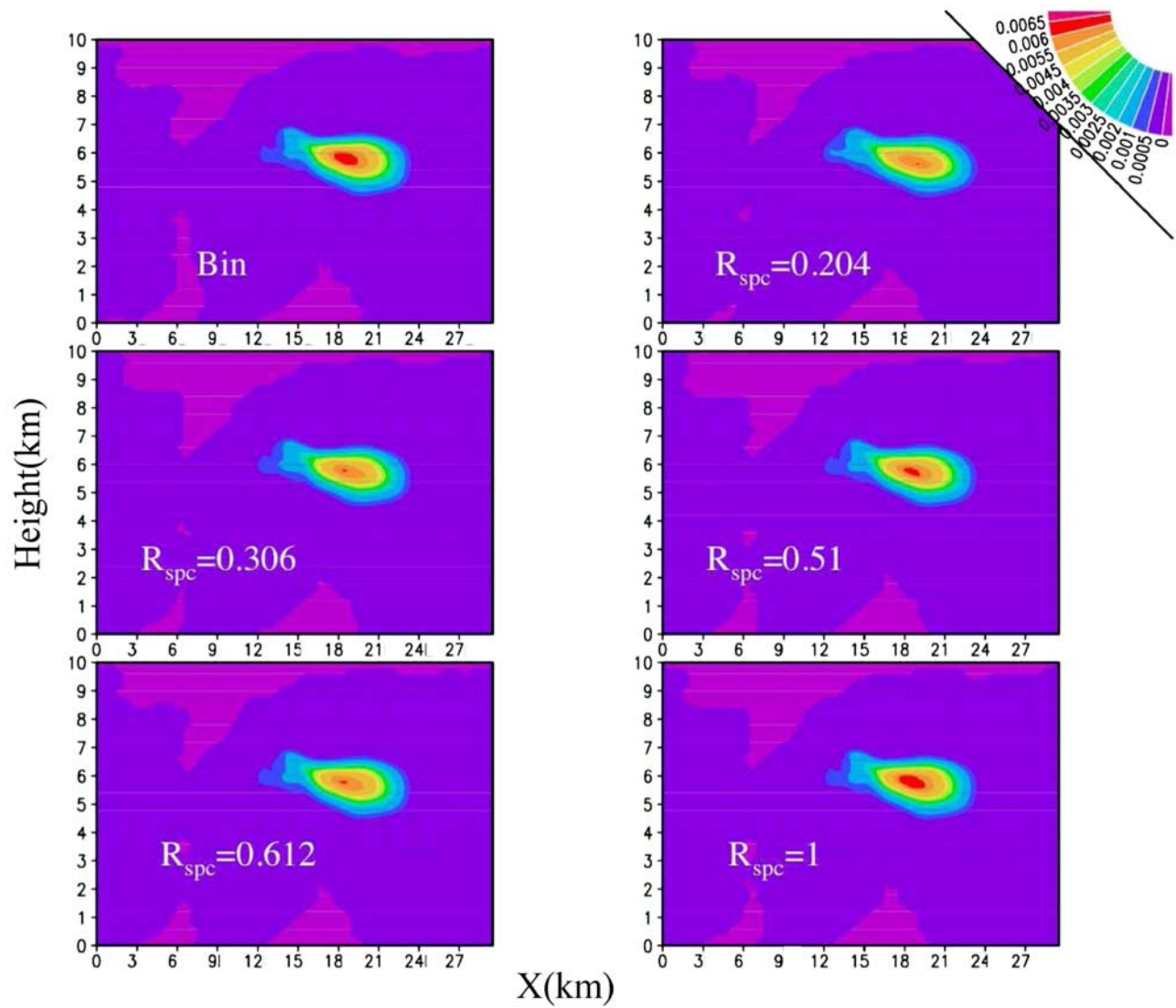


Figure 6. Horizontal distance-height sections of the amount of the snow water content integrated from $t = 0$ to the end of the calculation. Results for different values of R_{spc} are shown. The panel labeled with “bin” represents the result of the traditional bin model.

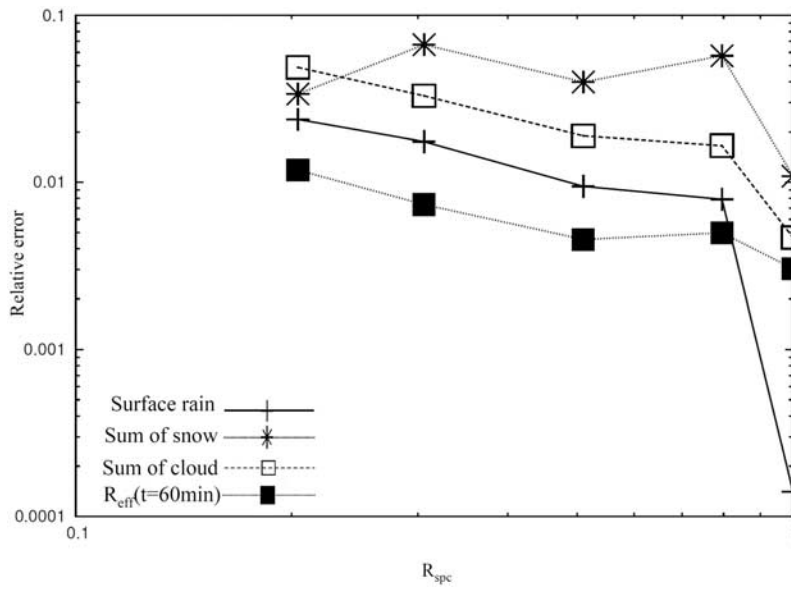


Figure 7. Same as Figure 5, but for results with various R_{spc} and $R = 0.124$.

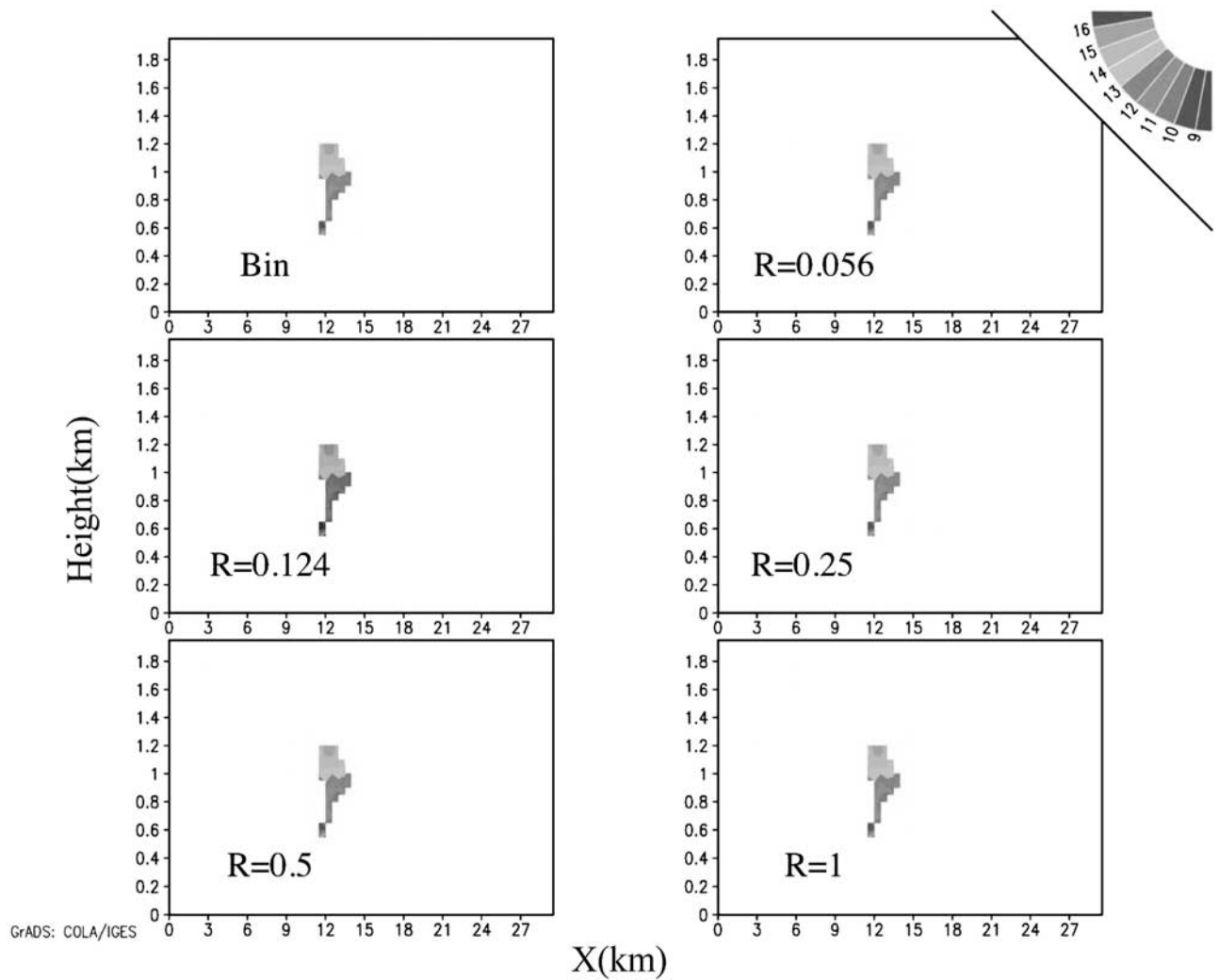


Figure 8. Same as Figure 4, but for the stratus case.

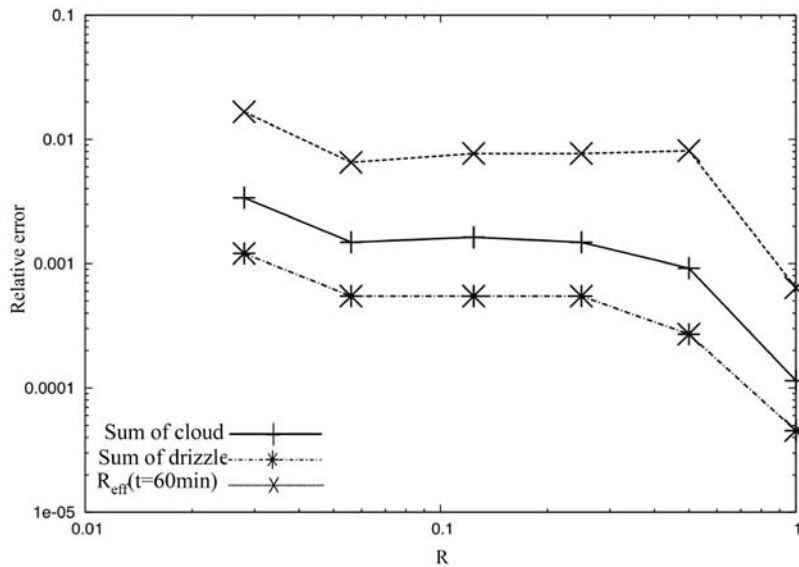


Figure 9. Same as Figure 5, but for the stratus case. Time-integrated amount of cloud water content (plusses), drizzle water content (asterisks), and effective radius at $t = 60$ min (crosses).

benefit of the MCI becomes in terms of the computational cost. For example, the MCI is better for simulation of thick stratus clouds and deep convective clouds.

[22] Furthermore, we evaluated how the simulation errors and standard deviations depend on the number of bins. We performed the same experiments as above but with 30 and 90 bins and compared the standard deviations and errors for the simulated cloud fields with those obtained from 60 bins. Figure 12 shows the error and the standard deviation of surface rainfall. The error has a similar trend regardless of the number of bins (Figure 12a), whereas the relative

standard deviation decreases with the number of bins (Figure 12b).

5. Application to a Numerical Weather Prediction Simulation (3-D Simulation)

[23] We apply the present MCI to a bin-type aerosol and cloud microphysics scheme in a framework of mesoscale model developed by *Iguchi et al.* [2008], which is a coupled model of the mesoscale operational model of the Japan Meteorological Agency [*Saito et al.*, 2006] with the Hebrew University Cloud Model (HUCM) [*Khain and Sednev*,

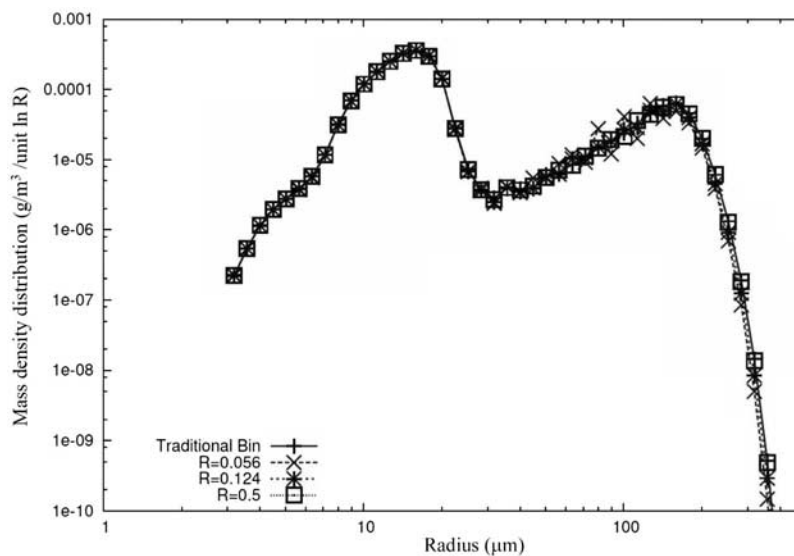


Figure 10. Spatially averaged mass density distribution (SDF) spectra (averaged over the spectra of the grid in which complex forms of spectra are calculated) in the stratus condition calculated by traditional bin (plusses) and our new method with $R = 0.056$ (crosses), 0.124 (asterisks), and 0.5 (squares).

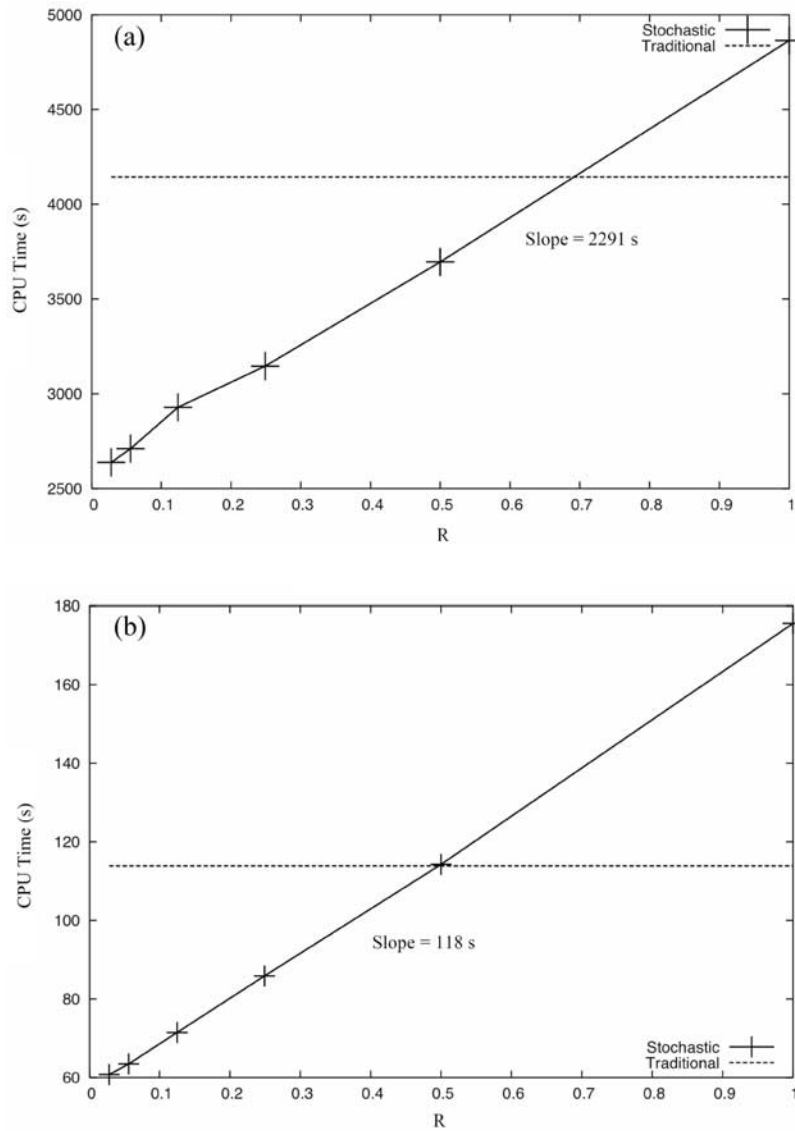


Figure 11. CPU time taken by the cloud microphysical module for the two-dimensional model simulation: CPU time in the (a) stratus case and (b) convective cloud case. CPU times for the MCI (crosses) and for the traditional bin method (solid line).

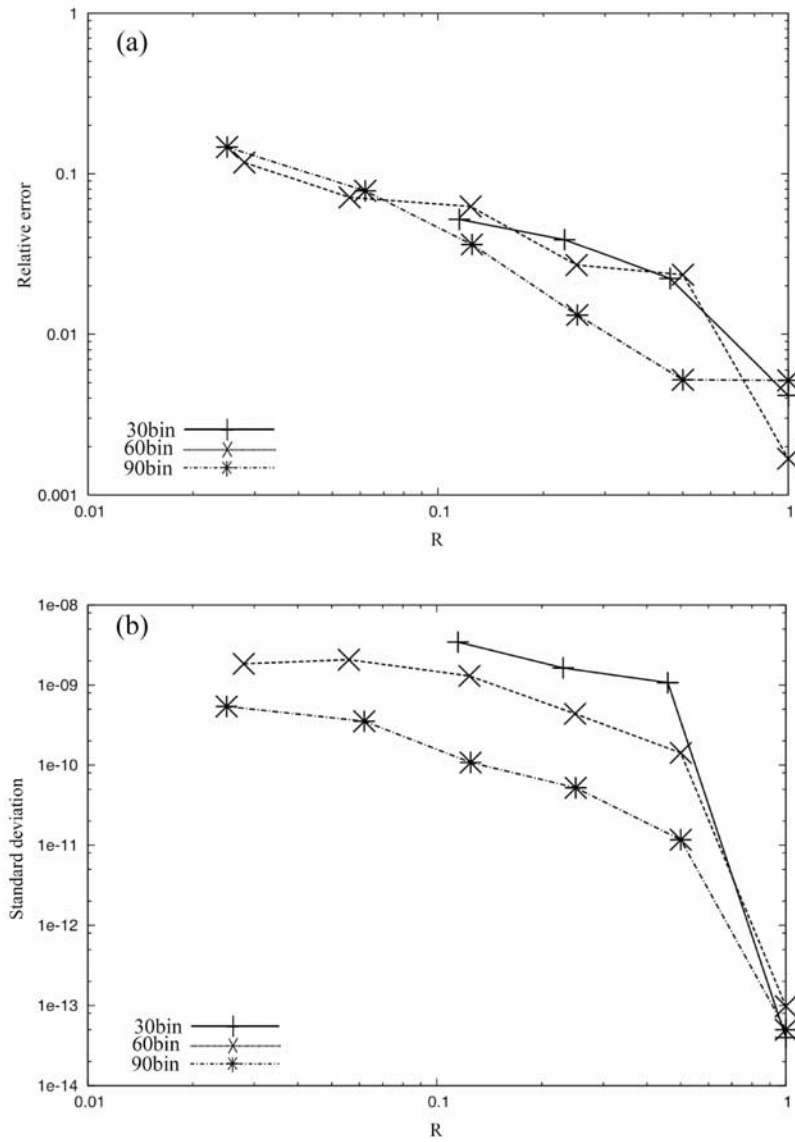


Figure 12. Errors and standard deviation of surface rain obtained by MCI for a various number of bins: (a) error and (b) standard deviation. Thirty bin (plusses), 60 bin (crosses), and 90 bin (asterisks).

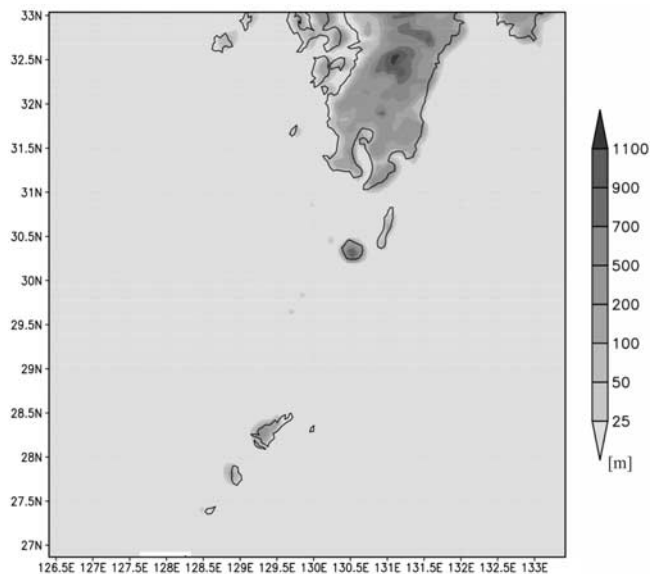


Figure 13. Calculation region for the numerical simulation by the NHM + HUCM model. Contours shows height (in meters) above sea level.

1996; *Khain et al.*, 2000]. This model includes nonhydrostatic dynamics, radiation and cloud microphysics. We show a very preliminary result of the cloud generated around the cold front. The simulation domain is a region around the East China Sea (125°E~134°E, 27°N~33°N) as shown in Figure 13. The horizontal resolution is 7 km and the SDFs of hydrometeors are discretized into 33 size bins on a uniform log-mass axis. R_{spc} at 1 and R at 0.056 have been set.

[24] The date of 8 April 2003 was selected for simulation, which is the same date simulated in *Iguchi et al.* [2008]. On

this day, a migrating low was located in the Japan Sea near the Korean Peninsula. This low activated a row of thick convective clouds from the center of the Japan Sea to the Naha and Taiwan region (see *Iguchi et al.* [2008] for general weather conditions of the day).

[25] Figure 14 shows the cloud optical thickness at 0300 UTC on 8 April 2003 simulated by the models with the stochastic (Figure 14b) and traditional bin methods (Figure 14a). The MCI generally produced the similar results to that by the traditional bin method. However, the difference between the two methods is larger in the areas where the clouds optical thickness is larger than in other area because the collision and coagulation processes are more active in the area. The error and CPU time for the numerical weather prediction simulation has a similar trend as in the preceding two-dimensional simulation as shown in Figure 15. For example, when R is 0.056, the relative error of the cloud optical thickness is about 7% and the CPU time of collision coagulation process is about 6% of traditional bin method.

6. Discussion

[26] In the preceding sections, we studied the behavior of errors produced by the present MCI in comparison with traditional bin method. In this section, we theoretically interpret the results shown above and further explore several aspects of the present method that would be beneficial for its potential applications in broader contexts.

6.1. Theoretical Survey of Collision Number

[27] Results obtained by the MCI contain random errors generated by seeded random numbers, and the variability of the results needs to be evaluated. Also, the collision-coagulation growth process in the real atmosphere is itself a random process and it is of some interest to compare the

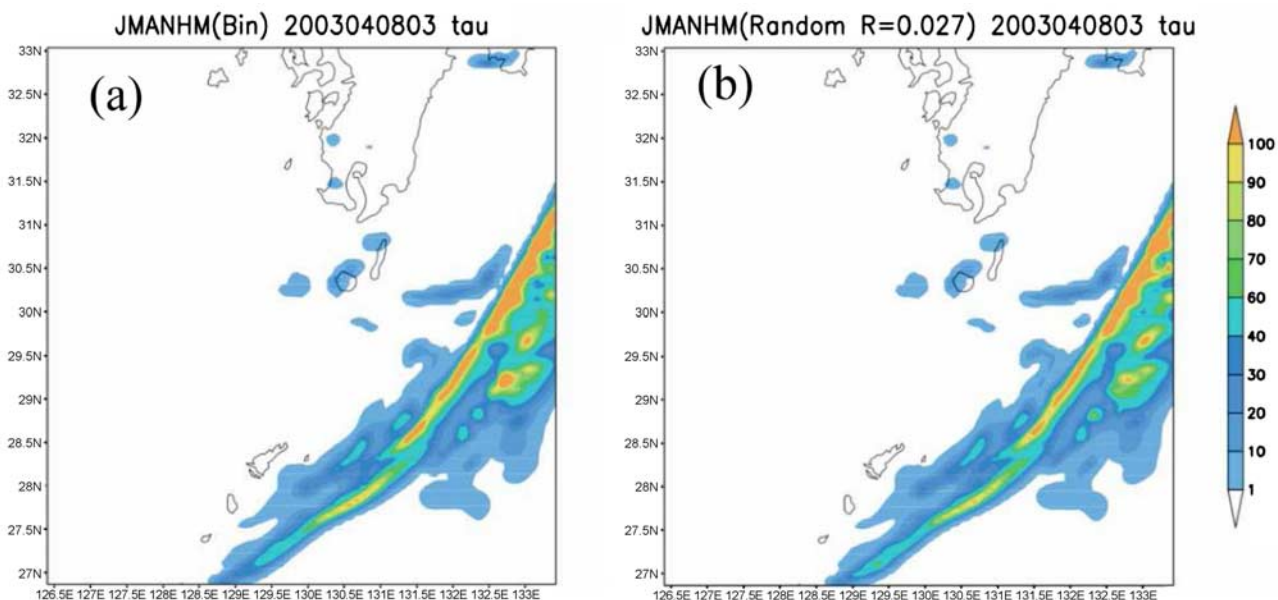


Figure 14. Horizontal distributions of cloud optical thickness at 0300 UTC, 8 April 2003, simulated by (a) the traditional bin method and (b) the MCI.

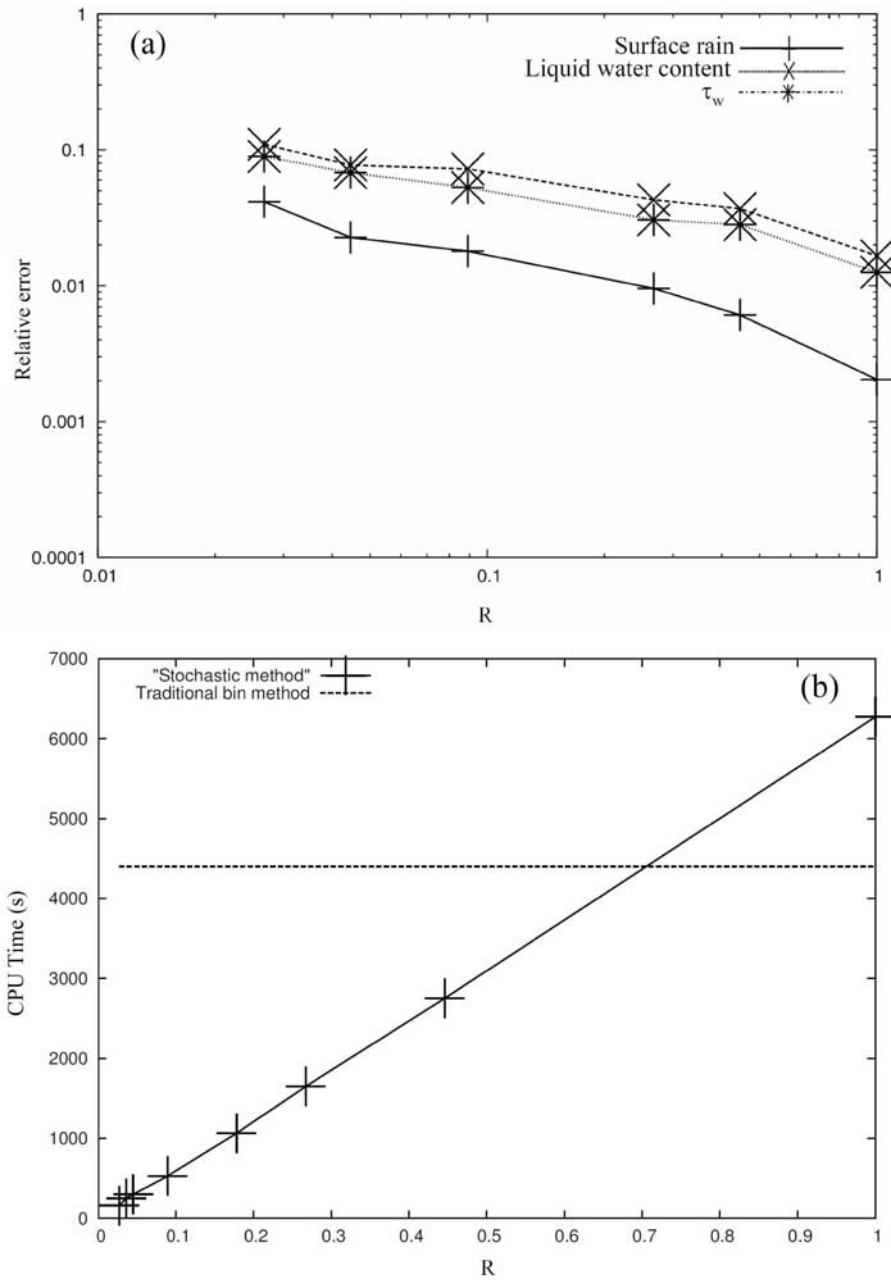


Figure 15. (a) Relative errors and (b) CPU times for the 3-D experiment with the MCI method implemented in the NHM + HUCM model. Figure 15a shows relative errors of surface rainfall (plusses), liquid water path (crosses), and optical thickness of water cloud (asterisks). Figure 15b shows CPU time of MCI taken by the collision and coagulation module for the 3-D experiment: MCI (crosses) and traditional bin method (solid line).

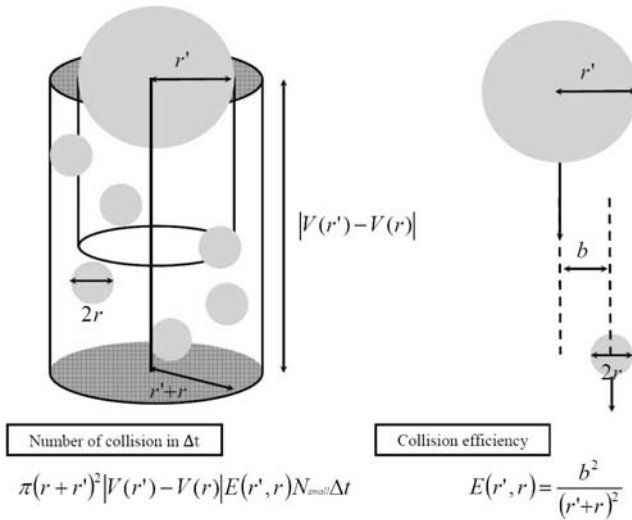


Figure 16. Schematic for the number of collisions in the atmosphere.

computational variability introduced by the MCI with the real variability.

[28] Reducing R is equivalent to decreasing the number of collisions in the model. Therefore, we can theoretically reduce R to the value corresponding to the number of collisions in real clouds. For example, if the number of collision in one grid is only ten, we can set the number of collision in the model to ten. For roughly evaluating this point, we use a very simple model shown in Figure 16. A large particle of hydrometeor with radius r' collects $M_{\text{collision}}$ small particles of hydrometeors with radius r as

$$M_{\text{collision}} = \pi(r+r')^2|V(r') - V(r)|E(r', r)N_{\text{small}}\Delta t,$$

$$E(r', r) = \frac{b^2}{(r'+r)^2},$$

where N_{small} is the number concentration of small particle of hydrometeors. Supposing that the number of large particle of hydrometeors is N_{large} , the number of collision $M'_{\text{collision}}$ between particles of radius r' and those of radius r is then given as

$$M'_{\text{collision}} = \pi(r+r')^2|V(r') - V(r)|E(r', r)N_{\text{small}}N_{\text{large}}\Delta t,$$

$$E(r', r) = \frac{b^2}{(r'+r)^2}.$$

[29] Table 2 lists the typical values of parameters for cloud, drizzle and rain that appear in this model [Rogers and Yau, 1989]. Assuming that $E(r', r)$ is 1, the values listed in Table 2 provide estimates for number of collisions, for example, between cloud droplets and raindrops as $10^4 \text{ m}^{-3} \text{ s}^{-1}$. Likewise, the number of collisions between cloud droplets and raindrops is approximately estimated as $10^7 \text{ m}^{-3} \text{ s}^{-1}$. The number of collisions between cloud droplets and drizzle drops is approximately given as $10^7 \text{ m}^{-3} \text{ s}^{-1}$ and the collision rate between drizzle particles and rain particles is approximately estimated as $10^4 \text{ m}^{-3} \text{ s}^{-1}$. Since one grid of our simulation is 10^4 m^3 (e.g., in

section 4), the number of collisions in the model is over 10^8 in one time step (1 s) in one grid. Therefore, we should theoretically set the number of collision M to $N_{\text{bin}}C_2$ (i.e., R set to one) for N_{bin} of 30, 60 and 90. This suggests that the present method can create errors if R is set to less than one.

6.2. Comparison of Monte Carlo Integration With Aircraft Data

[30] Next, we compared the computational errors with variability in aircraft observations that measure the SDF of clouds for investigating how comparable the numerical errors are to natural variabilities. This observed SDF is generally not a smooth function of a particle mass even if the cloud is relatively uniform. The nonsmooth nature of the SDF reflects the fact that the cloud parameters observed in real atmosphere fluctuate spatially and temporally due to the turbulent structure of the cloud. In order to compare variability of cloud parameters between simulation and observation, a stratus simulation was performed using the present MCI where variability of SDF in the results is caused by the random collision-coagulation process. The calculation domain is 30 km in horizontal ($dx = 0.2 \text{ km}$) and 5 km in vertical ($dz = 0.05 \text{ km}$). The integration time is 1 h with a time step of one second and R is set to 0.056. Initial conditions for temperature, horizontal wind and relative humidity are shown in Figure 17. Table 3 shows the spatially averaged mean and standard deviation of the effective radius by MCI in comparison with the values for corresponding parameters obtained by aircraft data and by the traditional bin model. Aircraft data were obtained by B200 aircraft for the JACCS aircraft project, which equipped the Gerber's microphysics probe PVM-100A [Gerber *et al.*, 1994]. On 2 February 1998, B200 flew in a region of $29 \pm 1\text{N}$, $128 \pm 1\text{E}$ with an average speed of about 80 m s^{-1} . Figure 18 shows effective radius of the aircraft observation data. The standard deviation of the effective radius from the MCI is the same order as that of aircraft observation data. Also, the mean values and standard deviations of the effective radius obtained by the traditional bin method are almost same as those by the MCI through cloud, drizzle and rain formation. These results demonstrate that both traditional bin and MCI can represent dispersion of cloud parameters obtained by observation and that the random error generated by MCI is much smaller than the variability included in the traditional bin model.

[31] This finding suggests that the model dispersion is the result of internal instability caused by the dynamics of the cloud system itself that takes place in the real atmosphere, which is much larger than the random error generated by the MCI. It can therefore be concluded that the dispersion

Table 2. Typical Values (Radius, Number Density, and Fall Velocity) of Cloud Droplet Drizzle Particles and Raindrops in the Atmosphere^a

	Radius (μm)	Number Density (cc^{-1})	Terminal Velocity (m/s)
Cloud	~ 10	$\sim 10^3$	$\sim 10^{-2}$
Drizzle	~ 100	~ 1	~ 1
Rain	~ 1000	$\sim 10^{-3}$	~ 10

^aFrom Rogers and Yau [1989].

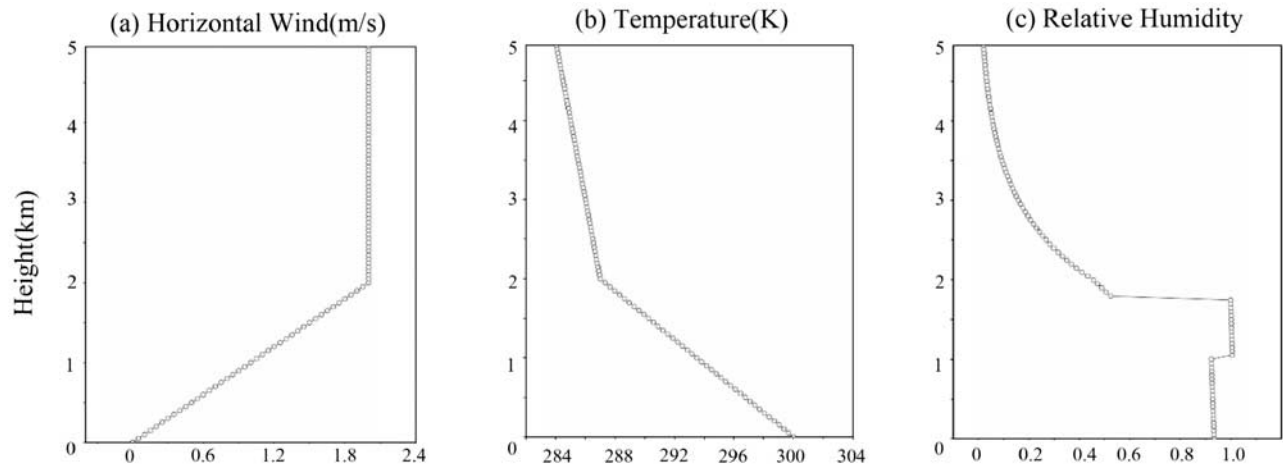


Figure 17. Initial conditions for atmospheric dynamics assumed for the two-dimensional numerical experiments: (a) horizontal wind, (b) temperature, and (c) relative humidity.

caused by the present MCI for the collision and coagulation process can be considered negligible compared to the natural variability in real atmosphere. This result supports the validity of the present MCI. It would also be interesting to compare the SDFs calculated by the MCI with those obtained from aircraft observations in terms of their randomness although such comparisons are difficult because observations always suffer errors in instrumentation as well as their random feature in nature.

[32] This article aims at development of a method to approximate the traditional bin scheme with focus on improvement of computational efficiency, and indeed demonstrated that the MCI is as accurate as the traditional bin models that have been compared with SDF observations by many investigators [e.g., *Khairoutdinov and Kogan, 1999*]. Although the comparisons of the model with direct observations of SDF by aircraft is out of the scope of this article, it is nevertheless worth noting that the natural cloud phenomenon with complicated size distribution functions cannot be fully reproduced even by traditional bin models as well as present MCI. This is a common issue open for cloud modeling community, for which we should keep making efforts.

6.3. Comparison With Bulk Method

[33] A main motivation of developing the MCI is to reduce computational cost and to speed up the bin model. In this regard, it is important to note that bulk models, widely used in cloud-resolving models, are much faster than bin models, and many works contributed to comparison of the bin model results with those of bulk models in terms of accuracy and computational efficiency [e.g., *Seifert et al., 2006*]. It is therefore useful for new parameterization of collision and coagulation process to compare the present MCI with results derived from the stochastic approach with those bulk parameterizations such as *Liu and Darm [2004]* and *Liu et al. [2007]* for the autoconversion process. According to a recent study of *Iguchi et al. [2008]*, there is not a large difference between bulk method and a bin method, to which our MCI was applied. This suggests that the MCI can reproduce similar results to bulk methods

although it is important to directly compare the present MCI with bulk methods in future studies.

6.4. Monte Carlo Integration as an Alternative Approach to Other Methods

[34] Traditional bin methods, when properly formulated, have important numerical characteristics that the numerical errors go to zero as the grid spacing and/or the time interval becomes zero. The present stochastic approach based on random sampling principle may be incompatible with these characteristics of bin methods. The particle-based method, which abandons the continuity of the size spectra, constitutes an alternative approach of modeling the microphysical processes. Although this method possesses several merits such as minimum advection errors and easy treatment of condensation processes, it still needs high computational cost and calculation resources especially when applied to multidimensional large domain simulations with fine resolutions. Our new approach proposed here provides another alternative approach to the traditional bin method and the particle-based method. And it provides an efficient approximation to bin methods that have been proven to simulate several important aspects of satellite-retrieved cloud microphysical properties.

7. Conclusions

[35] We proposed an application of the Monte Carlo integration procedure for the integration of the collision

Table 3. Values of Effective Radius and Its Standard Deviation Calculated by Each Model and Obtained by Aircraft Data^a

Model/Measurement	Effective Radius (μm)	Standard Deviation
Stochastic ($t = 25$ min)	11.776	0.30504
Traditional bin ($t = 25$ min)	11.778	0.30505
Stochastic ($t = 30$ min)	11.719	0.43937
Traditional bin ($t = 30$ min)	11.724	0.43915
Stochastic ($t = 40$ min)	9.2868	0.66117
Traditional bin ($t = 40$ min)	9.3037	0.66107
Aircraft	10.753	0.20896

^aIn the simulation, $t = 25$ min, 30 min, and 45 min correspond to the time for cloud, drizzle, and rain formation, respectively.

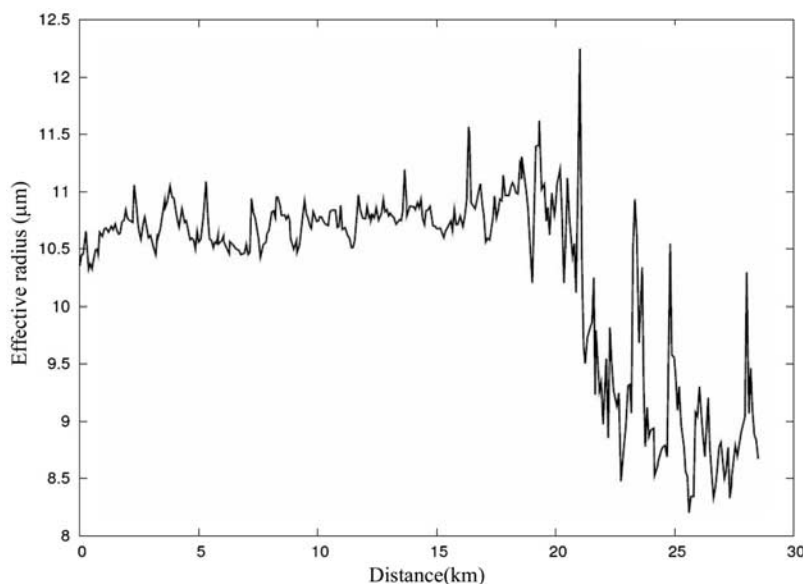


Figure 18. Values of effective radius as a function of the flight distance of B200 aircraft in the observation on 2 February 1998.

and coagulation equation of hydrometeor growth. This method reduces the computational cost of the collision and coagulation process to about 10% of that of the traditional method, thereby providing an efficient approximation of traditional bin method. This method employs uniformed random numbers, and it is shown that the results are dependent upon assumed random numbers. The random number principle causes some error, yet the error range of simulation results is found to be much less than internal variability that takes place in the real atmosphere.

[36] Although the present study focused only on collision-coagulation processes, it is also important to reduce the computational costs for condensational growth process that is another bottleneck in cloud microphysical modeling as shown in Table 1. Several previous studies were devoted to this issue [e.g., Bott, 1989a, 1989b; Lowe *et al.*, 2003; Suzuki, 2004] (T. Sugimura *et al.*, personal communication, 2008). We will also investigate how our stochastic approach can be applied to the condensational growth processes in future studies.

[37] **Acknowledgments.** We are grateful to M. Murakami of the Meteorological Research Institute of Japan for supplying aircraft data and to S. Shima of the JAMSTEC Earth Simulator Center for advice on the Monte Carlo integration. This research was supported by the Global Environment Research Fund B-4 of the Ministry of Environment, Japan, through project RR2002 and the Data Integration for Earth Observation project of the Ministry of Education, Sports, Science, Culture and Technology (MEXT) of Japan, and also by the JAXA/ADEOS-II GLI project.

References

- Berry, E. X. (1967), Cloud droplet growth by collection, *J. Atmos. Sci.*, *24*, 688–701, doi:10.1175/1520-0469(1967)024<0688:CDGBC>2.0.CO;2.
- Bott, A. (1989a), A positive definite advection scheme obtained by nonlinear renormalization of the advective fluxes, *Mon. Weather Rev.*, *117*, 1006–1015, doi:10.1175/1520-0493(1989)117<1006:APDASO>2.0.CO;2.
- Bott, A. (1989b), Reply to comment on “A positive definite advection scheme obtained by nonlinear renormalization of the advective fluxes,” *Mon. Weather Rev.*, *117*, 2633–2636, doi:10.1175/1520-0493(1989)117<2633:R>2.0.CO;2.
- Bott, A. (1998), A flux method for the numerical solution of the stochastic collection equation, *J. Atmos. Sci.*, *55*, 2284–2293, doi:10.1175/1520-0469(1998)055<2284:AFMFTN>2.0.CO;2.
- Bott, A. (2000), A flux method for the numerical solution of the stochastic collection equation: Extension to two-dimensional particle distributions, *J. Atmos. Sci.*, *57*, 284–294, doi:10.1175/1520-0469(2000)057<0284:AFMFTN>2.0.CO;2.
- Gallus, W. A., Jr., and M. Rancic (1996), A non-hydrostatic version of the NMC’s regional Eta model, *Q. J. R. Meteorol. Soc.*, *122*, 465–497.
- Gerber, H., B. G. Arends, and A. S. Ackerman (1994), New microphysics sensor for aircraft use, *Atmos. Res.*, *31*, 235–252, doi:10.1016/0169-8095(94)90001-9.
- Golovin, A. M. (1963), The solution of the coagulation equation for cloud droplets in a rising air current, *Bull. Acad. Sci. USSR, Geophys. Ser.*, *5*, 482–487.
- Iguchi, T., T. Nakajima, A. P. Khain, K. Saito, T. Takemura, and K. Suzuki (2008), Modeling the influence of aerosols on cloud microphysical properties in the east Asia region using a mesoscale model coupled with a bin-based cloud microphysics scheme, *J. Geophys. Res.*, *113*, D14215, doi:10.1029/2007JD009774.
- Khain, A. P., and I. Sednev (1996), Simulation of precipitation formation in the eastern Mediterranean coastal zone using a spectral microphysics cloud ensemble model, *Atmos. Res.*, *43*, 77–110, doi:10.1016/S0169-8095(96)00005-1.
- Khain, A. P., M. Ovchinnikov, M. Pinsky, A. Plkvovsky, and H. Krugliak (2000), Notes on the state-of-the-art numerical modeling of cloud microphysics, *Atmos. Res.*, *55*, 159–224, doi:10.1016/S0169-8095(00)00064-8.
- Khain, A., D. Rosenfeld, and A. Pokrovsky (2005), Aerosol impact on the dynamics and microphysics of deep convective clouds, *Q. J. R. Meteorol. Soc.*, *131*, 2639–2663, doi:10.1256/qj.04.62.
- Khairoutdinov, M. F., and Y. L. Kogan (1999), A large eddy simulation model with explicit microphysics: Validation against aircraft observations of a stratocumulus-topped boundary layer, *J. Atmos. Sci.*, *56*, 2115–2131, doi:10.1175/1520-0469(1999)056<2115:ALESMTW>2.0.CO;2.
- Liu, Y., and P. H. Darm (2004), Parameterization of the autoconversion process. Part I: Analytical formulation of the Kessler-type parameterizations, *J. Atmos. Sci.*, *61*, 1539–1548, doi:10.1175/1520-0469(2004)061<1539:POTAPI>2.0.CO;2.
- Liu, Y., P. H. Darm, R. L. McGraw, M. A. Miller, and S. Niw (2007), Theoretical expression for the autoconversion rate of the cloud droplet number concentration, *Geophys. Res. Lett.*, *34*, L16821, doi:10.1029/2007GL030389.
- Lowe, D., A. R. MacKenzie, N. Nikiforakis, and J. Kettleborough (2003), A condensed-mass advection based model for the simulation of liquid polar stratospheric clouds, *Atmos. Chem. Phys.*, *3*, 29–38.
- Lynn, B. H., A. P. Khain, J. Dudhia, D. Rosenfeld, A. Pokrovsky, and A. Seinfeld (2005), Spectral (bin) microphysics coupled with a mesoscale model (MM5). Part I: Model description and first results, *Mon. Weather Rev.*, *133*, 44–58, doi:10.1175/MWR-2840.1.

- Pruppacher, H., and J. D. Klett (1997), *Microphysics of Clouds and Precipitation*, 2nd ed., 954 pp., Springer, New York.
- Rogers, R. R., and M. K. Yau (1989), *A Short Course in Cloud Physics*, 3rd ed., 293 pp., Pergamon, Oxford, U. K.
- Rossow, W. B., and R. A. Schiffer (1999), Advances in understanding clouds from ISCCP, *Bull. Am. Meteorol. Soc.*, *80*, 2261–2287, doi:10.1175/1520-0477(1999)080<2261:AIUCFI>2.0.CO;2.
- Saito, K., et al. (2006), The operational JMA nonhydrostatic mesoscale model, *Mon. Weather Rev.*, *134*, 1266–1298, doi:10.1175/MWR3120.1.
- Seifert, A., A. Khain, A. Pokrovsky, and K. D. Beheng (2006), A comparison of spectral bin and two-moment bulk mixed-phase cloud microphysics, *Atmos. Res.*, *80*, 46–66, doi:10.1016/j.atmosres.2005.06.009.
- Shima, S., K. Kusano, A. Kawano, T. Sugiyama, and T. Kawahara (2009), Super-droplet method for the numerical simulation of clouds and precipitation: A particle-based and probabilistic microphysics model coupled with non-hydrostatic model, *Q. J. R. Meteorol. Soc.*, in press.
- Suzuki, K. (2004), A study on numerical modeling of cloud microphysics for calculating the particle growth process, Ph.D. thesis, Univ. of Tokyo.
- Suzuki, K., T. Nakajima, T. Y. Nakajima, and A. Khain (2006), Correlation pattern between effective radius and optical thickness of water clouds simulated by a spectral bin microphysics cloud model, *SOLA*, *2*, 116–119, doi:10.2151/sola.2006-030.
- Takahashi, T., and T. Kawano (1998), Numerical sensitivity study of rain-band precipitation and evolution, *J. Atmos. Sci.*, *55*, 57–87, doi:10.1175/1520-0469(1998)055<0057:NSSORP>2.0.CO;2.

T. Iguchi, T. Nakajima, and Y. Sato, Center for Climate System Research, University of Tokyo, Kashiwanoha 5-1-5, Kashiwa, Chiba 277-8568, Japan. (satoy@ccsr.u-tokyo.ac.jp)

K. Suzuki, Department of Atmospheric Science, Colorado State University, 1371 Campus Delivery, Fort Collins, CO 80523-1371, USA.